CHEMMEDCHEM

DOI: 10.1002/cmdc.200800383

# Fluorescent Benzofurazan–Cholic Acid Conjugates for in vitro Assessment of Bile Acid Uptake and Its Modulation by Drugs

Jana Rohacova,[a] M. Luisa Marín,[a] Alicia Martinez-Romero,[b] Laura Diaz,[b] José-Enrique O'Connor,[b] M. Jose Gomez-Lechon,[c, d] M. Teresa Donato,[c, d, e] José V. Castell,[c, d, e] and Miguel A. Miranda*[a]

*One of the most common mechanisms of hepatotoxicity is drug-induced cholestasis. Hence, new approaches for screening the cholestatic potential of drug candidates are desirable. In this context, we describe herein the use of synthetic 4-nitrobenzo-2-oxa-1,3-diazole (NBD) fluorescent conjugates of cholic acid (ChA) at positions 3α, 3β, 7α, and 7β for in vitro assessment of bile acid uptake. All the conjugates show a strong absorption band between 400 and 550 nm and have a fluorescence quantum yield of ~0.45, with an emission maximum centered at ~530 nm. After their photophysical characterization, 3α-, 3β-, 7α-, and 7β-NBD–ChA were used to monitor uptake in freshly isolated rat hepatocytes by means of a previously optimized flow cytometry technique. Transport of the cholic acid derivatives inside the cell was detected and quantified by measuring the increase of NBD green fluorescence within cells over time. The effect of troglitazone, a well-known inhibitor of bile acid uptake by the sodium taurocholate co-transporting polypeptide, supports the specificity of fluorescent NBD–ChA transport. According to the final intracellular fluorescence level attained and the uptake rate, 3α-NBD–ChA was found to be the most efficient derivative. Furthermore, sodium valproate, cyclosporin A, and chlorpromazine decreased the uptake of 3α-NBD–ChA, in agreement with their relative in vivo potency as cholestatic compounds; in contrast, sodium citrate (the negative control) had no effect. These results support the suitability of the in vitro flow cytometric assay with NBD–ChA to detect compounds that affect bile acid uptake.*

## Introduction

Continuous bile formation is an important function of the liver. Transport of solutes from blood to bile is driven by several active systems in both sinusoidal and canalicular membranes of hepatocytes. Drug-induced cholestasis is a common mechanism of hepatotoxicity.[1]

Chemical inhibition of transport across the canalicular membrane may cause intracellular accumulation of bile acids in hepatocytes and subsequent toxicity due to membrane alterations, mitochondrial dysfunction, and cellular necrosis.[2–4] A major goal for the pharmaceutical industry is to provide safer drugs with fewer side effects; hence it is desirable to disregard compounds that exhibit cholestatic properties early in the preclinical phases of the drug-development process. For this purpose, new methods and approaches for screening the cholestatic potential of drug candidates are required.[5,6] Freshly isolated rat hepatocytes are good in vitro models to examine bile acid uptake and its modulation by drugs.[7,8] We previously reported an optimized flow cytometry assay for the study of bile acid transport in hepatocytes using cholylamidofluorescein (CamF), a fluorescent derivative of cholic acid (ChA).[9] This allowed us to demonstrate that CamF is taken up by living rat hepatocytes in a concentration-dependent fashion. However, further studies have shown that CamF is much bulkier than ChA and lacks the negative charge at the side chain, which may affect its specific transport through the main bile acid transporters in the hepatocyte membrane.

To overcome these problems it seemed convenient to use a smaller fluorophore and to keep the acid moiety at the lateral chain.[10] In this context, the benzofurazan moiety introduces only small structural changes on the main nucleus.[11,12] Thus, several 4-nitrobenzo-2-oxa-1,3-diazole (NBD)-amino conjugates of cholic acid have already been prepared and used for fluorescence microscopy studies.[13,14] For instance, it has been dem-

[a] *J. Rohacova, Dr. M. L. Marín, Prof. Dr. M. A. Miranda*
*Instituto de Tecnología Química, Departamento de Química (UPV-CSIC)*
*Avda. de los Naranjos s/n, 46022 Valencia (Spain)*
*Fax: (+34) 963877809*
*E-mail: mmiranda@qim.upv.es*

[b] *Dr. A. Martinez-Romero, L. Diaz, Dr. J.-E. O'Connor*
*Laboratorio de Citómica, Unidad Mixta CIPF-UVEG*
*Centro de Investigación Príncipe Felipe*
*Avda. Autopista del Saler 16-3, 46013 Valencia (Spain)*

[c] *Dr. M. J. Gomez-Lechon, Dr. M. T. Donato, Prof. Dr. J. V. Castell*
*Unidad de Hepatología Experimental*
*Centro de Investigación Hospital Universitario "La Fe"*
*Avda. Campanar, 46009 Valencia (Spain)*

[d] *Dr. M. J. Gomez-Lechon, Dr. M. T. Donato, Prof. Dr. J. V. Castell*
*CIBERHEPAD, FIS (Spain)*

[e] *Dr. M. T. Donato, Prof. Dr. J. V. Castell*
*Departamento de Bioquímica y Biología Molecular*
*Facultad de Medicina, Universidad de Valencia*
*Avda. Blasco Ibáñez, 46020 Valencia (Spain)*

Supporting information for this article is available on the WWW under http://dx.doi.org/10.1002/cmdc.200800383.

onstrated that 7β-NBD–cholyltaurine is taken up by isolated rat hepatocytes through the same transport systems as the parent nonfluorescent compound.[15–17]

We describe herein the use of synthetic NBD–ChA fluorescent derivatives at positions 3α, 3β, 7α, or 7β (Figure 1). After their photophysical characterization these compounds were checked to monitor uptake in hepatocytes using the flow cytometry technique previously optimized by us.[9] The use of troglitazone, a well-known inhibitor of bile acid uptake by the sodium taurocholate co-transporting polypeptide,[18] supports the specificity of the transport of our fluorescent derivatives. The suitability of the flow cytometric assay with NBD–ChA to detect compounds that affect bile acid uptake in vitro was also demonstrated in this study.

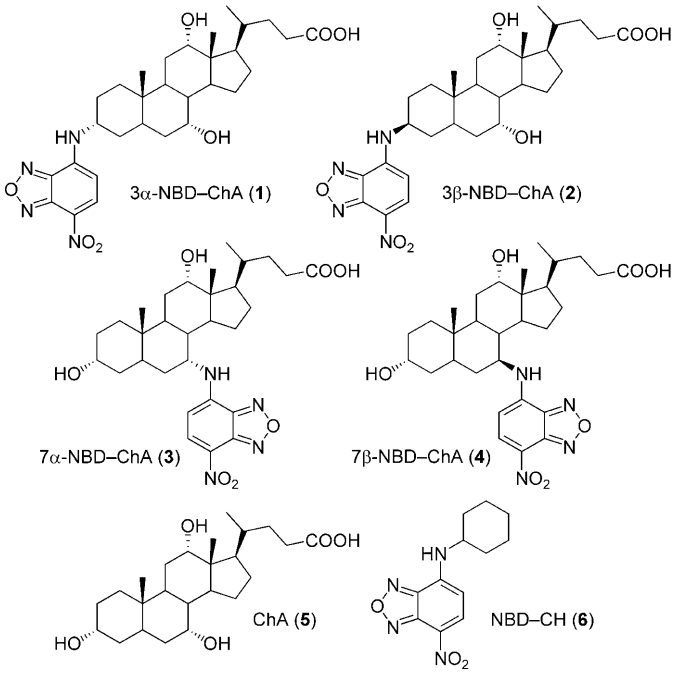


**Figure 1.** Structures of bile acid derivatives.

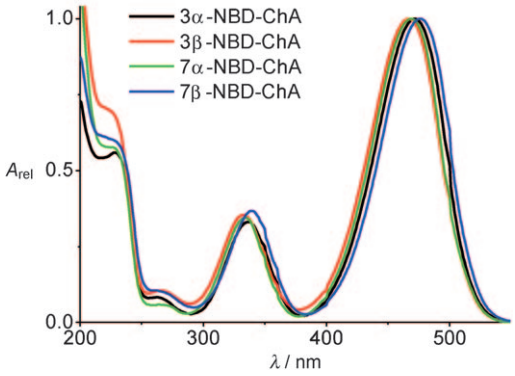


**Figure 2.** Normalized absorption spectra of the four NBD–ChA derivatives **1**–**4** in ethanol.

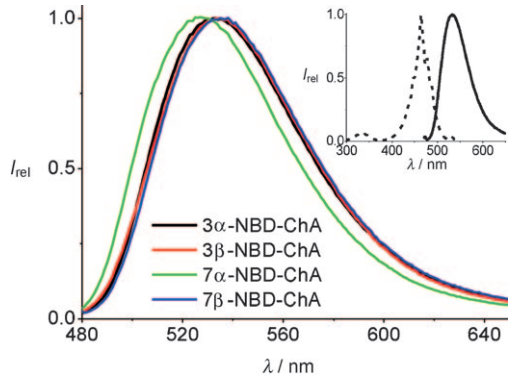


**Figure 3.** Fluorescence emission spectra of 3α-, 3β-, 7α-, and 7β-NBD–ChA in ethanol obtained after excitation at $\lambda_{max}$ (nm) under nitrogen. The inset shows the excitation–emission spectra of 3α-NBD–ChA (**1**) as a representative case.

## Results and Discussion

### Photophysical measurements

The UV/Vis absorption spectra of the four NBD derivatives in ethanol exhibit maxima at ~330 and 470 nm (Figure 2). The only significant deviation was observed with 7β-NBD–ChA (**4**), maxima of which were red-shifted by ~5 nm.

The fluorescence emission spectra of **1**, **2**, and **4** in ethanol show a broad maximum at ~537 nm (in every case, $\lambda_{ex}$ corresponds to the absorption maxima at ~470 nm), whereas the maximum corresponding to the 7α-NBD–ChA isomer **3** was blue-shifted to 531 nm (see Figure 3 and Table 1). These results are very similar to those reported previously for the corresponding taurine-conjugated NBD derivatives in ethanol.[13] No significant changes were observed when the measurements were performed in the presence of oxygen. From the intersection of the corresponding normalized excitation and emission spectra of the four derivatives, singlet energy ($E_{0-0}$) values of ~242 kJ mol$^{-1}$ were estimated. By means of time-resolved fluorescence spectroscopy, lifetimes ($\tau_S$) of ~6 ns in ethanol were determined for the four compounds. To complete the characterization of the singlet excited states of the four conjugates, fluorescence quantum yields were measured. The values obtained were ~40%, as shown in Table 1. A model compound possessing the NBD fluorophore attached to cyclohexane but lacking the complex steroidal skeleton (compound **6**) was prepared and used to confirm the photophysical properties of **1**–**4**. As can be seen in Table 1, the singlet excited state of this model showed the same behavior as the cholic acid derivatives.

In contrast to the singlet state properties, the photophysical behavior of triplets has received less attention. However, these longer-lived transient species provide a wider dynamic range, which could be potentially useful for analytical purposes. Hence, in our hands, triplet transient states ($\lambda_{max}$ ~390 nm) were obtained for the four isomers in ethanol (see Supporting Information).[19]

  

**Table 1.** Photophysical characteristics of the singlet excited state of the NBD conjugates.

| Compound | $\lambda_{abs}$ [nm] | $\lambda_{em}$ [nm] | $\phi_F$[a] | $E_S$ [kJ mol$^{-1}$]/[kcal mol$^{-1}$] | $\tau_S$ [ns] |
|---|---|---|---|---|---|
| 3α-NBD–ChA (**1**) | 471 | 537 | 0.47 | 241/57.7 | 5.9 |
| 3β-NBD–ChA (**2**) | 467 | 537 | 0.44 | 242/57.8 | 6.2 |
| 7α-NBD–ChA (**3**) | 469 | 531 | 0.47 | 243/58.2 | 5.6 |
| 7β-NBD–ChA (**4**) | 476 | 537 | 0.51 | 240/57.4 | 6.4 |
| NBD–CH (**6**) | 468 | 537 | 0.46 | 241/57.7 | 6.3 |

[a] Determined with fluorescein in an ethanolic solution of KOH (0.01 M) as reference ($\phi_F = 0.97$).

### Flow cytometry experiments

To assess the suitability of the four different NBD–ChA fluorescent conjugates for bile acid uptake, the dynamics of this process across the plasma membrane was investigated in fresh suspensions of rat hepatocytes. For this purpose, multi-parametric flow cytometry was applied, as it allows the examination of multiple fluorescence emissions of individual cells in suspension in real time. This strategy was recently used to demonstrate the specific uptake of CamF, the fluorescent bile acid scaffold mentioned above.[9] Thus, in the initial series of experiments a flow cytometric kinetic assay of the uptake was performed in real time on the first derivative of the series, namely 3α-NBD–ChA. Cell suspensions were stained with propidium iodide for 5 minutes prior to flow cytometric analysis to identify and gate out dead cells (Figure 4 A). In this way, the specific uptake by live cells was followed by a kinetic plot of green fluorescence intensity versus time (Figure 4 B). The results show that living hepatocytes accumulated 3α-NBD–ChA slowly but constantly over the course of the 5-minute experimental period.

In a second series of experiments the dependence of 3α-NBD–ChA transport on the operation of bile acid transporters in the plasma membrane of liver cells was addressed (Figure 5). Uptake of bile acids by hepatocytes is mediated mostly by the sodium taurocholate co-transporting polypeptide (Ntcp), which is responsible for the sodium-dependent uptake process. Bile acid uptake is also mediated, but to a much lesser extent, by the organic anion transporting polypeptide family (OATP), which is responsible for basolateral uptake.[20] Troglitazone, a hepatotoxic thiazolidinedione formerly used for the treatment of non-insulin-dependent diabetes mellitus, is an in vivo cholestatic compound[21] that is a strong in vitro inhibitor of bile acid uptake through Ntcp and OATP in both suspended and sandwich-cultured rat hepatocytes.[18] Thus, as Figure 5 shows, pre-incubation of fresh hepatocyte suspensions with troglitazone provoked a strong and dose-dependent decrease in the rate of 3α-NBD–ChA uptake, in accordance with previous data obtained with similar troglitazone concentrations, but on a different assay system.[18] Because the results are consistent with a transporter-mediated, troglitazone-inhibited uptake of 3α-ChA, characterization of the other fluorescent derivatives was attempted with a similar experimental design. For this purpose, fresh suspensions of rat hepatocytes were pre-incubated with troglitazone or vehicle, and then the uptake kinetics of each individual NBD derivative was examined by flow cytometry for a period of up to 30 minutes.

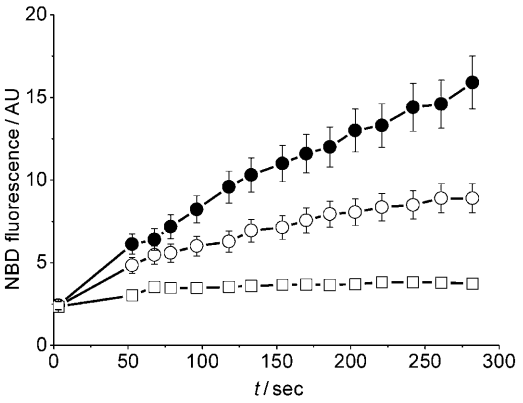


**Figure 5.** Effect of the bile acid transport inhibitor troglitazone (●: 0 μM, ○: 1 μM, □: 10 μM) on the uptake of fluorescent NBD–bile acid conjugate 3α-NBD–ChA by rat hepatocytes. The graphs show the kinetics of the fluorescence mean intensity in live cells at the indicated times.

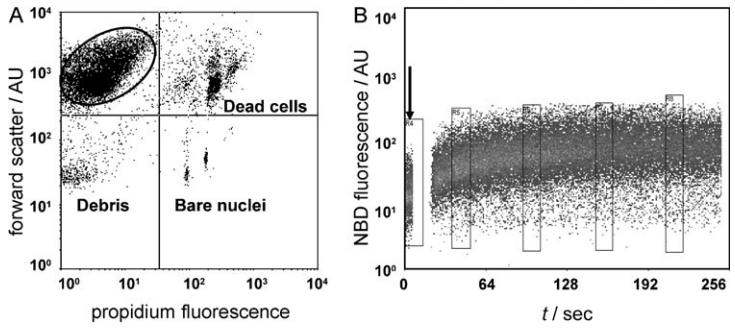


**Figure 4.** Flow cytometric analysis of the uptake of fluorescent NBD–bile acid conjugate 3α-NBD–ChA by rat hepatocytes. A) Selection of live cells for the analysis; live cells are delimited by the elliptical gate shown in the upper left quadrant. B) Kinetics of 3α-NBD–ChA uptake by live rat hepatocytes. Transport of 3α-NBD–ChA inside the cell was detected and quantified by measuring the increase of green fluorescence in cells over time. Rectangular regions shown along the *x* axis indicate analytical regions for mathematical calculations from raw cytometric data.

As shown in Figure 6, troglitazone-treated liver cells did not exhibit a significant uptake of the fluorescent bile acids in all cases, while untreated hepatocytes accumulated the NBD–ChA derivative slowly but constantly until a plateau was reached, about 20 minutes following addition. Quantitative differences between the NBD derivatives were observed in the general uptake trend in a comparison of the individual plots. Thus, both the initial uptake rate and the final intracellular fluorescence level attained allowed a classification of the apparent efficiency of the NBD–ChA conjugates in the order: 3α-NBD > 3β-NBD ≈ 7α-NBD > 7β-NBD. More interestingly, the ki-

  

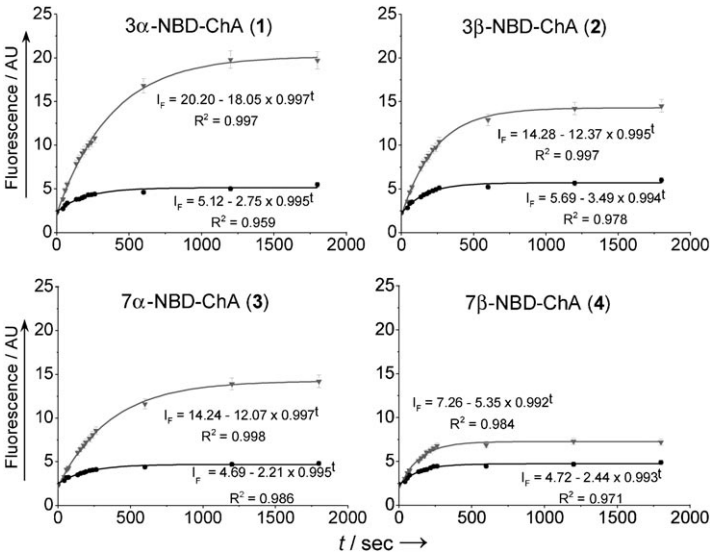


**Figure 6.** Comparative kinetics of the uptake of four related fluorescent NBD–bile acid conjugates (as indicated) by rat hepatocytes in the presence (●) and absence (▼) of troglitazone. The graphs show the kinetics of fluorescence mean intensity in live cells along with the corresponding equations and regression coefficients.

netic plot of the increase of mean fluorescence intensity ($I_F$) fitted well with an equation of the type $I_F = a - b \times c^t$, in which $a$ represents the maximum fluorescence intensity reached and $a-b$ is the basal cell autofluorescence prior to addition of the NBD derivative (Figure 6). The uptake rate in arbitrary NBD fluorescence units per second was calculated as the first derivate when 50% of the maximum fluorescence intensity was reached. According to this criterion, the uptake rates of 3α-NBD–ChA and 3β-NBD–ChA were very close to each other (0.027 and 0.031) and faster than that of 7α-NBD–ChA (0.018) and 7β-NBD–ChA (0.021). Remarkably, the uptake rate in the presence of troglitazone strongly decreased in all cases (between 0.005 and 0.010). As expected, the basal autofluorescence was always similar.

The above observations on the initial uptake rate of the various NBD derivatives and the effect of troglitazone suggest that these probes may be used to detect and quantify toxic effects related to bile acid uptake by suspended hepatocytes. The combination of NBD-derived fluorescent probes and flow cytometry measurements may be a powerful tool for in vitro assessment of bile acid uptake. However, real-time kinetic experiments by flow cytometry become unpractical when a large number of compounds or a wide range of concentrations are to be tested, owing to both the excessive instrument time required and compromised viability of suspended hepatocytes during extended periods. Because the uptake kinetics of all the assayed NBD derivatives shows stable and consistent intracellular accumulation for at least 30 min, single end-point measurements of intracellular NBD fluorescence might be adequate to detect exogenous effects on bile acid uptake. In this way, a larger throughput could be achieved. As a proof of concept of this design, we analyzed the effects of several known cholestatic compounds on the accumulated intracellular NBD fluorescence after 15 min incubation with 3α-NBD–ChA, the most efficient derivative of this family. For this series of experiments chlorpromazine and cyclosporin A, two strong cholestatic compounds,[22,23] and sodium valproate, a weak cholestatic[22] but with reported in vivo cholestasis activity,[24] were tested in a range of sub-cytotoxic concentrations. Sodium citrate was used as a non-cholestatic negative control. Figure 7 shows that, according to their relative potency as cholestasis-inducing agents, both chlorpromazine and cyclosporin A induce marked

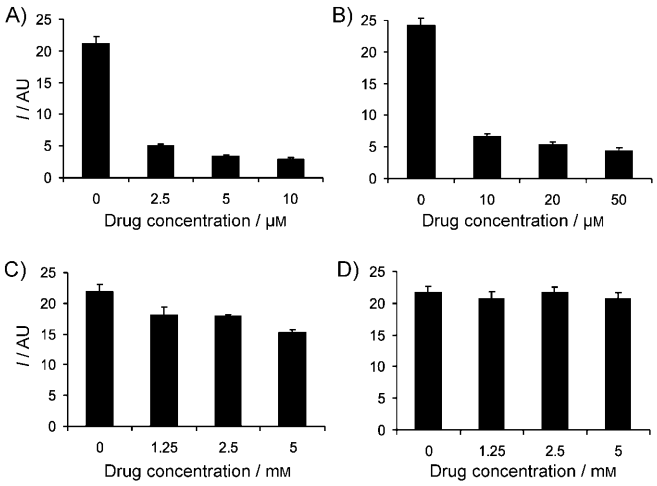


**Figure 7.** Effect of three bile acid transport inhibitors A) chlorpromazine, B) cyclosporin A and C) sodium valproate, and D) negative control (sodium citrate) on the uptake of 3α-NBD–ChA by rat hepatocytes. Cell suspensions were pre-incubated with test compounds and stained with propidium iodide prior to the addition of 3α-NBD–ChA (100 nM) and further incubation for 15 min. The mean fluorescence intensity of NBD in live cells was then determined by flow cytometry.

decreases in intracellular NBD fluorescence at all concentrations tested, whereas sodium valproate induces only a small decrease in NBD fluorescence at the highest concentration used. Sodium citrate, the negative control, did not cause any significant variation in NBD intracellular accumulation.

## Conclusions

Four synthetic 7-nitrobenzo-2-oxa-1,3-diazole (NBD) fluorescent conjugates of cholic acid at positions 3α, 3β, 7α, and 7β were prepared and characterized. Their photophysical properties make them adequate for monitoring uptake in freshly isolated rat hepatocytes using a previously optimized flow cytometry technique.

We recently reported an optimized flow cytometry kinetic assay for studies of bile acid transport in suspended hepatocytes based on the fluorescent derivative cholylamidofluorescein (CamF).[9] In the work presented herein, this flow cytometric strategy is extended to characterize the kinetics and specificity of the uptake of four different fluorescent NBD–ChA derivatives. Whereas intracellular transport of the cholic acid derivatives can be detected and quantified by measuring the time-dependent increase in NBD green fluorescence in cells, single

  

end-point measurements of cellular fluorescence allow determination of the maximal concentration reached and the stability of the intracellular accumulation of the NBD–ChA fluorescent conjugates.

The effect of troglitazone, a well-known inhibitor of Ntcp, the main transporter of bile acids into hepatocytes,[20] has allowed us to demonstrate both the suitability and specificity of the four NBD derivatives for analysis of bile acid uptake in fresh suspended rat hepatocytes. In all cases, there was a strong decrease in the uptake rate by troglitazone, showing that the kinetic approach may be useful for a rapid and quantitative characterization of drug effects on bile acid uptake by rat suspended hepatocytes.

To overcome the disadvantages that may hamper kinetic experiments by flow cytometry in miniaturized and automated assays with a larger throughput,[25] we performed single end-point measurements of intracellular NBD fluorescence. In this way, the effects of several known cholestatic compounds on the uptake of 3α-NBD–ChA, the most efficient fluorescent derivative, were tested. Our results show that sodium valproate, cyclosporin A, and chlorpromazine decrease the uptake of the NBD fluorescent conjugate according to their relative in vivo potency as cholestatic compounds, while sodium citrate (the negative control) shows no effect. These results support the applicability of the end-point flow cytometric assay with 3α-NBD–ChA to detect compounds that affect bile acid uptake in vitro. It should be emphasized that in these end-point measurements, data from only 10000 cells were acquired, which, under our experimental conditions, represents an approximate volume of 100 μL of the original hepatocyte suspension. At a typical acquisition rate of 500–1000 cells per second in a flow cytometer, obtaining a single data point may take 10 to 20 seconds. Thus, both the small number of cells required and the speed of data generation are fully compatible with assay miniaturization in a 96-well plate format, and make the assay amenable to automation using multi-well-sampling flow cytometers,[25] thus increasing analytical throughput in pharmacological and toxicological studies.

## Experimental Section

### *Chemicals*

Cholic acid, NBD-Cl, collagenase, DMSO, and propidium iodide were supplied by Sigma Chemical Co. (Madrid, Spain) and used as received. Ethanol (99.9%) was obtained from Merck (Darmstadt, Germany). Ham's F-12 and Lebovitz L-15 media, and calf serum were purchased from Gibco (Madrid, Spain). Chlorpromazine, cyclosporin A, sodium valproate, troglitazone, and all other chemicals used for the synthesis of the fluorescent derivatives were obtained reagent grade from Sigma–Aldrich and were used as received.

NBD derivatives **1**–**4** were prepared as previously described.[13] The same experimental procedure was also applied for the preparation of NBD–CH (**6**). A complete NMR spectroscopic characterization ($^1$H and $^{13}$C) is included for all (see below).

### *Characterization*

The $^1$H and $^{13}$C NMR spectra were measured with a Bruker (Rheinstetten, Germany) 300 MHz instrument; $CDCl_3$ and $CD_3OD$ were used as solvents, and the signal corresponding to the solvent in each case was taken as reference: $CDCl_3$ ($\delta = 7.26$ ppm for $^1$H NMR, $\delta = 77.2$ ppm for $^{13}$C NMR); $CD_3OD$ ($\delta = 3.31$ ppm for $^1$H NMR, $\delta = 49.0$ ppm for $^{13}$C NMR). Coupling constants are given in Hz. Exact mass spectra are included for all compounds (see below).

***N*-(7-nitro-2,1,3-benzoxadiazol-4-yl)-3α-amino-7α,12α-dihydroxy-5β-cholan-24-oic acid (3α-NBD–ChA)** (**1**): $^1$H NMR (300 MHz, $CD_3OD$): $\delta = 0.74$ (s, 3H, Me-18), 1.00 (s, 3H, Me-19), 1.03 (d, $J = 6.3$ Hz, 3H, Me-21), 3.64 (m, 1H, $CH_{ax}$-3), 3.82 (s, 1H, $CH_{eq}$-7), 3.99 (s, 1H, $CH_{eq}$-12), 6.37 (d, $J = 8.7$ Hz, 1H, $CH_{Ar}$-6′), 8.50 ppm (d, $J = 8.7$ Hz, 1H, $CH_{Ar}$-5′); $^{13}$C NMR (75 MHz, $CD_3OD$): $\delta = 178.4$ (COOH), 145.8 ($C_{Ar}$), 145.7 ($C_{Ar}$), 138.6 (CH-5′), 122.4 ($C_{Ar}$), 99.8 (CH-6′), 73.9 (CH-12), 68.9 (CH-7), 47.5 (CH), 43.5 (CH), 43.1 (CH), 41.1 (CH), 36.9 (CH), 36.8 ($CH_2$), 36.0 (C), 35.7 ($CH_2$), 32.4 ($CH_2$), 32.1 ($CH_2$), 29.6 ($CH_2$), 28.7 ($CH_2$), 28.1 (CH), 24.2 ($CH_2$), 23.2 ($CH_3$), 17.6 ($CH_3$), 13.0 ppm ($CH_3$); HRMS *m/z* 570.3046 (calcd for $C_{30}H_{42}N_4O_7$ 570.3055).

***N*-(7-nitro-2,1,3-benzoxadiazol-4-yl)-3β-amino-7α,12α-dihydroxy-5β-cholan-24-oic acid (3β-NBD–ChA)** (**2**): $^1$H NMR (300 MHz, $CD_3OD$): $\delta = 0.73$ (s, 3H, Me-18), 1.03 (m, 6H, Me-19+Me-21), 2.82 (d t, $J = 14.9$ Hz, 1H), 3.83 (br s, 1H, $CH_{eq}$-7), 3.99 (br s, 1H, $CH_{eq}$-12), 4.14 (br s, 1H, $CH_{eq}$-3), 6.39 (d, $J = 9$ Hz, 1H, $CH_{Ar}$-6′), 8.51 ppm (d, $J = 9$ Hz, 1H, $CH_{Ar}$-5′); $^{13}$C NMR (75 MHz, $CD_3OD$): $\delta = 180.2$ (COOH), 147.3 ($C_{Ar}$), 146.7 ($C_{Ar}$), 138.2 (CH-5′), 122.0 ($C_{Ar}$), 99.7 (CH-6′), 74.0 (CH-12), 69.0 (CH-7), 47.6 (CH), 43.0 (CH), 41.0 (CH), 38.4 (CH), 37.0 (CH), 36.3 (C), 35.4 ($CH_2$), 33.7 ($CH_2$), 33.0 ($CH_2$), 32.2 ($CH_2$), 29.8 ($CH_2$), 28.7 ($CH_2$), 27.7 (CH), 24.2 ($CH_2$), 23.4 ($CH_3$), 17.7 ($CH_3$), 13.0 ppm ($CH_3$); HRMS *m/z* 570.3057 (calcd for $C_{30}H_{42}N_4O_7$ 570.3055).

***N*-(7-nitro-2,1,3-benzoxadiazol-4-yl)-7α-amino-3α,12α-dihydroxy-5β-cholan-24-oic acid (7α-NBD–ChA)** (**3**): $^1$H NMR (300 MHz, $CD_3OD$): $\delta = 0.77$ (s, 3H, Me-18), 1.03 (m, 6H, Me-19+Me-21), 3.39 (m, 1H, $CH_{ax}$-3), 3.99 (br s, 1H, $CH_{eq}$-7), 4.05 (br s, 1H, $CH_{eq}$-12), 6.36 (d, $J = 9$ Hz, 1H, $CH_{Ar}$-6′), 8.55 ppm (d, $J = 9$ Hz, 1H, $CH_{Ar}$-5′); $^{13}$C NMR (75 MHz, $CD_3OD$): $\delta = 178.5$ (COOH), 146.2 ($C_{Ar}$), 145.3 ($C_{Ar}$), 138.6 (CH-5′), 123.4 ($C_{Ar}$), 100.0 (CH-6′), 73.9 (CH-12), 72.3 (CH-3), 52.6 (CH-7), 47.8 (CH), 43.3 (CH), 42.8 (CH), 40.0 ($CH_2$), 38.3 (CH), 36.7 (CH), 36.2($CH_2$), 32.3 ($CH_2$), 32.1 ($CH_2$), 31.0 ($CH_2$), 30.8 ($CH_2$), 29.5 ($CH_2$), 28.3 ($CH_2$), 24.1 ($CH_2$), 22.8 ($CH_3$), 17.7 ($CH_3$), 12.7 ppm ($CH_3$); HRMS *m/z* 570.3064 (calcd for $C_{30}H_{42}N_4O_7$ 570.3055).

***N*-(7-nitro-2,1,3-benzoxadiazol-4-yl)-7β-amino-3α,12α-dihydroxy-5β-cholan-24-oic acid (7β-NBD–ChA)** (**4**): $^1$H NMR (300 MHz, $CD_3OD$): $\delta = 0.79$ (s, 3H, Me-18), 1.01 (d, $J = 6.3$ Hz, 3H, Me-21), 1.04 (s, 3H, Me-19), 3.57 (m, 1H, $CH_{ax}$-3), 3.83 (m, 1H, $CH_{ax}$-7), 3.98 (br s, 1H, $CH_{eq}$-12), 6.30 (d, $J = 9$ Hz, 1H, $CH_{Ar}$-6′), 8.54 ppm (d, $J = 9$ Hz, 1H, $CH_{Ar}$-5′); $^{13}$C NMR (75 MHz, $CD_3OD$): $\delta = 178.3$ (COOH), 146.1 (C), 145.6 (C), 139.0 (CH-5′), 122.2 (C), 98.7 (CH-6′), 73.1 (CH-12), 72.1 (CH-3), 55.1 (CH-7), 49.2 (CH), 46.8 (CH), 43.4 (CH), 41.5 (CH), 37.3 ($CH_2$), 36.6 (CH), 36.1($CH_2$), 34.8 (C), 34.5 ($CH_2$), 34.1 (CH), 32.3 ($CH_2$), 32.1 ($CH_2$), 30.9 ($CH_2$), 30.3 ($CH_2$), 28.9 ($CH_2$), 26.7 ($CH_2$), 23.6 ($CH_3$), 17.6 ($CH_3$), 13.3 ppm ($CH_3$); HRMS *m/z* 570.3062 (calcd for $C_{30}H_{42}N_4O_7$ 570.3055).

***N*-(7-nitro-2,1,3-benzoxadiazol-4-yl)-cyclohexylamine (NBD–CH)** (**6**): $^1$H NMR (300 MHz, $CDCl_3$): $\delta = 1.54$ (m, 5H, *c*Hex), 1.74 (m, 1H), 1.87 (m, 2H), 2.17 (m, 2H), 3.67 (m, 1H, CH-NH), 6.19 (d, $J = 8.7$ Hz, 1H, $CH_{Ar}$-6′), 8.47 ppm (d, $J = 8.7$ Hz, 1H, $CH_{Ar}$-5′); $^{13}$C NMR (75 MHz, $CDCl_3$): $\delta = 144.5$ ($C_{Ar}$), 144.1 ($C_{Ar}$), 143.0 ($C_{Ar}$), 136.7 (CH-5′), 123.7

  

($C_{Ar}$), 98.8 (CH-6′), 53.0 (CH), 32.4 ($CH_2$), 25.2 ($CH_2$), 24.7 ppm ($CH_2$); HRMS *m/z* 262.1073 (calcd for $C_{12}H_{14}N_4O_3$ 262.1066).

### *Photophysical measurements*

Absorption measurements (UV/Vis) were performed on a Jasco V-530 spectrometer (Japan). Fluorescence spectra were recorded on an FS900 fluorimeter, and lifetimes were measured with an FL900 setup, both from Edinburgh Instruments (Reading, UK). Lifetime measurements were based on single photon counting using a hydrogen flash lamp (1.5 ns pulse width) as the excitation source. The kinetic traces were fitted by single-exponential decay functions using a re-convolution procedure to separate from the lamp pulse profile. The solutions were purged with $N_2$ for at least 15 min before the measurements. The absorbance of the solutions at the excitation wavelength was kept $<0.1$. Cuvettes of 1 cm optical path length were used, and experiments were performed in absolute EtOH at room temperature.

### *Flow cytometry analysis of the NBD–ChA uptake by hepatocytes*

Hepatocytes were obtained from 200–300 g Sprague–Dawley male rats by perfusion of the liver with collagenase as described elsewhere.[26] Cell viability of suspensions, assessed by the trypan blue exclusion test, was $>85\,\%$.

All kinetic and single end-point measurements were performed in triplicate using a Cytomics FC500 MCL flow cytometer (Beckman–Coulter, Brea, CA, USA) equipped with an air-cooled argon-ion laser emitting at 488 nm. The fluorescence emissions were collected at 525 nm (NBD green fluorescence) and 625 nm (propidium iodide orange fluorescence). Measurements of forward angle laser light scatter (FS), an estimation of cell size, were used for gross morphological assessment of hepatocytes and the exclusion of debris. Data analysis in the kinetic and single end-point flow cytometric measurements was performed using CXP software (Beckman–Coulter) interfaced with the flow cytometer. Similar results were obtained in an EPICS XL flow cytometer (Beckman–Coulter).

The uptake kinetics of the various NBD–ChA derivatives was evaluated by flow cytometry as previously described.[9] Suspensions of freshly isolated rat hepatocytes were diluted at $10^5$ viable cells per mL in Ham's F-12/Lebovitz L-15 (1:1) medium supplemented with 2% calf serum plus 0.2% bovine serum albumin and kept at 37 °C in a 5% $CO_2$ humidified atmosphere until analysis. Flow cytometric experiments were always performed within 2 h after cell isolation. Hepatocyte suspensions were dispensed in standard polypropylene tubes and stained with propidium iodide at a final concentration of 5 $\mu g\,mL^{-1}$ for 5 min to identify and exclude dead cells from the analysis. Detector settings were adjusted to display live cells as the events with largest forward scatter and lowest orange fluorescence (corresponding to autofluorescence). Live cells were thus delimited by and selected according to the elliptical gate shown in the upper left quadrant. Dead and dying cells appear as intense propidium fluorescent events, while bare nuclei released by necrotic cells appear as small but fluorescent events. At the starting time, each tube was loaded in the flow cytometer, and data acquisition was maintained for ~10 s in order to detect the green autofluorescence of cells. Data acquisition was then paused, and an appropriate volume of stock solution (1 $mg\,mL^{-1}$ in EtOH) of the corresponding NBD derivative was added quickly to the tube for a final concentration of 100 nM. From this moment, data acquisition was continued for 300 s. Transport of the cholic acid derivative inside the cell can be detected and quantified by measuring the increase of NBD green fluorescence in cells over time. For this purpose, rectangular analytical regions are implemented by the cytometer-interfaced computer along the graph *x* axis to obtain mathematical values from the raw cytometric data.

Single end-point flow cytometric measurements of cellular fluorescence were performed to determine the maximal concentration and the stability of intracellular fluorescence accumulation. Following the initial kinetic measurement, each treated sample was run again in the flow cytometer at 10, 20, and 60 min after addition of the NBD derivative. In these end-point measurements, fluorescence data from 10000 live cells were acquired.

To check for specificity, hepatocyte suspensions were treated with troglitazone, a well-known cholestatic drug, which inhibits bile salt uptake and efflux.[18] Dilute hepatocyte suspensions were incubated for 15 min at 37 °C with troglitazone (10 μM final concentration from a stock solution at 1 $mg\,mL^{-1}$ in DMSO) or an appropriate volume of DMSO. Uptake kinetics for NBD fluorescence was then determined by flow cytometry as described above.

The effect of model compounds with described in vitro cholestatic action of strong (chlorpromazine and cyclosporin A) or moderate (sodium valproate) intensity was also tested.[22–24] For this purpose, diluted hepatocyte suspensions were incubated for 15 min with either cholestatic compound at increasing concentrations or a similar volume of DMSO. Following initial drug treatment, each sample was treated with 3α-NBD–ChA (100 nM) and run again in the flow cytometer after 15 min. In these end-point measurements, fluorescence data from 10000 live cells were acquired.

## *Acknowledgements*

*Financial support from CSIC (fellowship I3P-2005), the European Commission (LSHB-CT-2004-504761 and LSHB-CT-2004-512051), the Spanish Government (BIO2007-65662 and RIRAAF RETICS), and the Generalitat Valencia (Prometeo program) is gratefully acknowledged.*

**Keywords:** chlorpromazine · cholestasis · flow cytometry · hepatocytes · troglitazone

[1] G. Abboud, N. Kaplowitz, *Drug Saf.* **2007**, *30*, 277–294.
[2] N. M. Delzenne, P. B. Calderon, H. S. Taper, M. B. Roberfroid, *Toxicol. Lett.* **1992**, *61*, 291–304.
[3] G. J. Gores, H. Miyoshi, R. Botla, H. I. Aguilar, S. F. Bronk, *Biochim. Biophys. Acta Bioenerg.* **1998**, *1366*, 167–175.
[4] A. P. Rolo, C. M. Palmeira, J. M. Holy, K. B. Wallace, *Toxicol. Sci.* **2004**, *79*, 196–204.
[5] M. Horikawa, Y. Kato, C. A. Tyson, Y. Sugiyama, *Drug Metab. Pharmacokinet.* **2003**, *18*, 16–22.
[6] T. L. Marion, E. M. Leslie, K. L. Brouwer, *Mol. Pharmacol.* **2007**, *4*, 911–918.
[7] M. McConkey, H. Gillin, C. R. Webster, M. S. Anwer, *J. Biol. Chem.* **2004**, *279*, 20882–20888.
[8] R. Kubitz, N. Saha, T. Kühlkamp, S. Dutta, S. Vom Dahl, M. Wettstein, D. Häussinger, *J. Biol. Chem.* **2004**, *279*, 10323–10330.
[9] J. Rohacova, M. L. Marín, A. Martinez-Romero, J. E. O'Connor, M. J. Gomez-Lechon, M. T. Donato, J. V. Castell, M. A. Miranda, *Photochem. Photobiol. Sci.* **2008**, *7*, 860–866.
[10] C. D. Schteingart, S. Eming, H. T. Ton-Nu, D. L. Crombie, A. F. Hofmann in *Bile Acids and the Hepatobiliary System* (Eds.: G. Paumgartner, W. Gerok, A. Stiehl), London: Kluwer Academic, **1992**, 177–183.

  

[11] R. R. Rando, F. W. Bangerter, M. R. Alecio, *Biochim. Biophys. Acta Biomembr.* **1982**, *684*, 12–20.
[12] J. A. Monti, S. T. Christian, W. A. Shaw, W. H. Finley, *Life Sci.* **1977**, *21*, 345–356.
[13] S. Schneider, U. Schramm, A. Schreyer, H.-P. Buscher, W. Gerok, G. Kurz, *J. Lipid Res.* **1991**, *32*, 1755–1767.
[14] U. Schramm, A. Dietrich, S. Schneider, H.-P. Buscher, W. Gerok, G. Kurz, *J. Lipid Res.* **1991**, *32*, 1769–1779.
[15] U. Schramm, G. Fricker, H.-P. Buscher, W. Gerok, G. Kurz, *J. Lipid Res.* **1993**, *34*, 741–757.
[16] W. Kramer, G. Kurtz, *J. Lipid Res.* **1983**, *24*, 910–923.
[17] W. Kramer, S. Schneider, *J. Lipid Res.* **1989**, *30*, 1281–1288.
[18] D. C. Kemp, M. J. Zamek-Gliszczynski, K. L. Brouwer, *Toxicol. Sci.* **2005**, *83*, 207–214.
[19] S. Uchiyama, K. Takchira, S. Kohtani, K. Imai, R. Nakagaki, S. Tobita, T. Santa, *Org. Biomol. Chem.* **2003**, *1*, 1067–1072.
[20] M. Trauner, J. L. Boyer, *Phys. Rev.* **2003**, *83*, 633–671.
[21] C. Funk, C. Ponelle, G. Scheuermann, M. Pantze, *Mol. Pharmacol.* **2001**, *59*, 627–635.
[22] R. B. Kim, B. Leake, M. Cvetkovic, M. M. Roden, J. Nadeau, A. Walubo, G. R. Wilkinson, *J. Pharmacol. Exp. Ther.* **1999**, *291*, 1204–1209.
[23] S. Mita, H. Suzuki, H. Akita, H. Hayashi, R. Onuki, A. F. Hofmann, Y. Sugiyama, *Drug Metab. Dispos.* **2006**, *34*, 1575–1581.
[24] M. Fayad, R. Choueiri, M. Mikati, *J. Child Neurol.* **2000**, *15*, 135–136.
[25] L. A. Sklar, M. B. Carter, B. S. Edwards, *Curr. Opin. Pharmacol.* **2007**, *7*, 527–534.
[26] M. J. Gomez-Lechon, R. Jover, T. Donato, X. Ponsoda, C. Rodriguez, K. G. Stenzel, R. Klocke, D. Paul, I. Guillen, R. Bort, J. V. Castell, *J. Cell. Physiol.* **1998**, *177*, 553–562.

Received: November 12, 2008
Revised: December 10, 2008
Published online on January 27, 2009

  